We are IntechOpen,
the world's leading publisher of
Open Access books
Built by scientists, for scientists

5,500
Open access books available

136,000
International authors and editors

170M
Downloads

154
Countries delivered to

Our authors are among the

TOP 1%
most cited scientists

12.2%
Contributors from top 500 universities

BOOK CITATION INDEX
CLARIVATE ANALYTICS
INDEXED

WEB OF SCIENCE™

Selection of our books indexed in the Book Citation Index
in Web of Science™ Core Collection (BKCI)

Interested in publishing with us?
Contact book.department@intechopen.com

Numbers displayed above are based on latest data collected.
For more information visit www.intechopen.com

Analysis of the Electrochemical Transport Properties of Doped Barium Cerate for Proton Conductivity in Low Humidity Conditions: A Review

Laura I.V. Holz, Vanessa C.D. Graça,
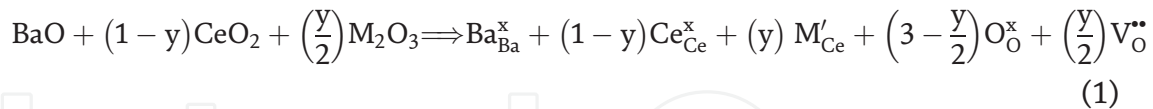*Francisco J.A. Loureiro and Duncan P. Fagg*

Abstract

Proton-conducting perovskites are among the most promising electrolytes for Proton Ceramic Fuel Cells (PCFCs), electrolysers and separation membranes. Particularly, yttrium-doped barium cerate, $BaCe_{1-x}Y_xO_{3-\delta}$ (BCY), shows one of the highest protonic conductivities at intermediate temperatures ($\sigma \sim 10^{-3}$ S cm^{-1} at 400°C); values that are typically achieved under humidified atmospheres ($p_{H2O} \sim 10^{-2}$ atm). However, BCY has commonly been discarded for such applications due to its instability in the presence of water vapour and carbonaceous atmospheres. A recent discovery has shown that BCY10 exhibits pure protonic conductivity under very low humidity contents ($\sim 10^{-5}$–10^{-4} atm), owing to its very high equilibrium constant for hydration. This peculiar characteristic allows this material to retain its functionally as a proton conductor in such conditions, while preventing its decomposition. Hence, this chapter explores the electrochemical properties of the $BaCe_{0.9}Y_{0.1}O_{3-\delta}$ (BCY10) composition, comprehensively establishing its limiting operation conditions through defect chemistry and thermodynamic analyses. Moreover, the importance of such conditions is highlighted with respect to potential industrially relevant hydrogenation/de-hydrogenation reactions at low temperatures under low humidity.

Keywords: perovskite, barium cerate, protonic conductivity, transport number, nominally dry conditions

1. Introduction

Ceramic proton conductors have been highlighted for electrochemical synthesis, as potential membranes in hydrogenation and dehydrogenation reactions [1]. One of the best compositions for this role is that of the doped barium cerate, *e.g.* $BaCe_{1-x}M_xO_{3-\delta}$ (M = Y^{3+}, In^{3+}, Gd^{3+}, etc.), which can show very high levels of proton conductivity at intermediate temperatures (*i.e.* $\sigma \sim 10^{-3}$ S cm^{-1} at 400°C) [2–9]. This material belongs to the perovskite family with ABO_3 ceramic oxide

structure, including a divalent alkaline earth element, such as Ba^{2+} (also, Sr^{2+} or Ca^{2+}), in the A-cation site, while a tetravalent rare-earth element, Ce^{4+}, is present in the B-cation site. The introduction of dopants in the B-site with suitable acceptor elements, such as Y^{3+}, In^{+3} or Gd^{3+} trivalent cations, leads to the formation of charge compensating oxygen vacancies [9]:

$$BaO + (1-y)CeO_2 + \left(\frac{y}{2}\right)M_2O_3 \Longrightarrow Ba_{Ba}^x + (1-y)Ce_{Ce}^x + (y)\,M'_{Ce} + \left(3 - \frac{y}{2}\right)O_O^x + \left(\frac{y}{2}\right)V_O^{\bullet\bullet}$$
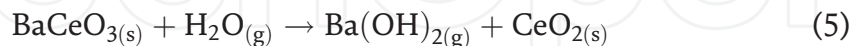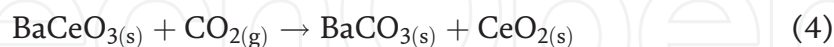
(1)

In addition to potential oxide-ion conductivity, these acceptor-substituted materials are also capable of offering both protonic and electronic conductivity, depending on the temperature and atmospheric conditions. The protonic conductivity is the most significant characteristic of these materials that is usually associated with the existence of protonic defects ($OH_O^{\bullet}$), upon filling of these oxygen vacancies in the presence of water vapour, as expressed by Eq. (2) [10–13]:

$$H_2O + V_O^{\bullet\bullet} + O_O^x \Leftrightarrow 2OH_O^{\bullet}$$

(2)

Accordingly, the equilibrium constant for hydration, K_w, is given by the following equation:

$$K_w \approx \frac{[OH_O^{\bullet}]^2}{p_{H2O}[V_O^{\bullet\bullet}][O_O^x]}$$

(3)

Due to the significant importance of humidity to promote protonic conductivity, most of the reported studies of barium cerate based materials have focused on highly wetted atmospheres with typical water vapour partial pressure $p_{H2O} \sim 3 \times 10^{-2}$ atm [14–18]. Unfortunately, these works also underline the tendency of this material for reacting with acidic gases, *viz.* carbon dioxide (CO_2) and water vapour (H_2O), leading to the formation of insulating carbonate or hydroxide phases, respectively, on the surface of the material. This complication impedes the ability of this material to be used in highly humidified and carbon-based fuels, thus, limiting its potential application range [3, 14–20]. The typical degradation reactions in such atmospheres include:

$$BaCeO_{3(s)} + CO_{2(g)} \rightarrow BaCO_{3(s)} + CeO_{2(s)}$$

(4)

$$BaCeO_{3(s)} + H_2O_{(g)} \rightarrow Ba(OH)_{2(g)} + CeO_{2(s)}$$

(5)

The chemical stability of doped barium cerates is well documented in the literature and huge efforts have been made to explore the reasons behind its chemical instability, using both conventional and non-conventional techniques [21–25]. For instance, Matsumoto *et al.* [22] studied the effect of dopant M in $BaCe_{0.9}M_{0.1}O_{3-\delta}$ (M = Y, Tm, Yb, Lu, In, or Sc) on the electrical conductivity in the temperature range 400–900°C and on the chemical stability with respect to CO_2 by thermogravimetry (TG). Both the electrical conductivity (moistened H_2 or O_2, $p_{H2O} = 1.9 \times 10^{-2}$ atm) and the stability against carbonate formation were shown to decrease with increasing ionic radius (**Figure 1**), corresponding to an increase in basicity. Nonetheless, all compounds were found to interact with pure CO_2 at temperatures below 900°C, failing to succeed in the mitigation of the chemical instability in the doped barium cerate.
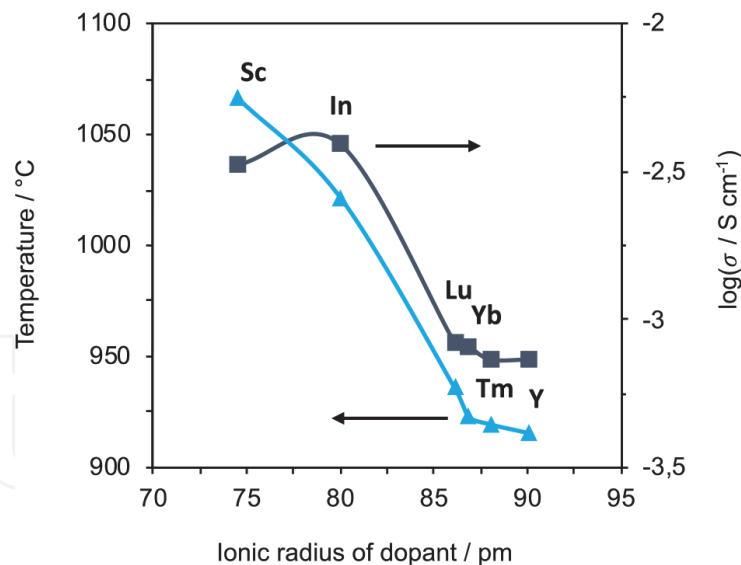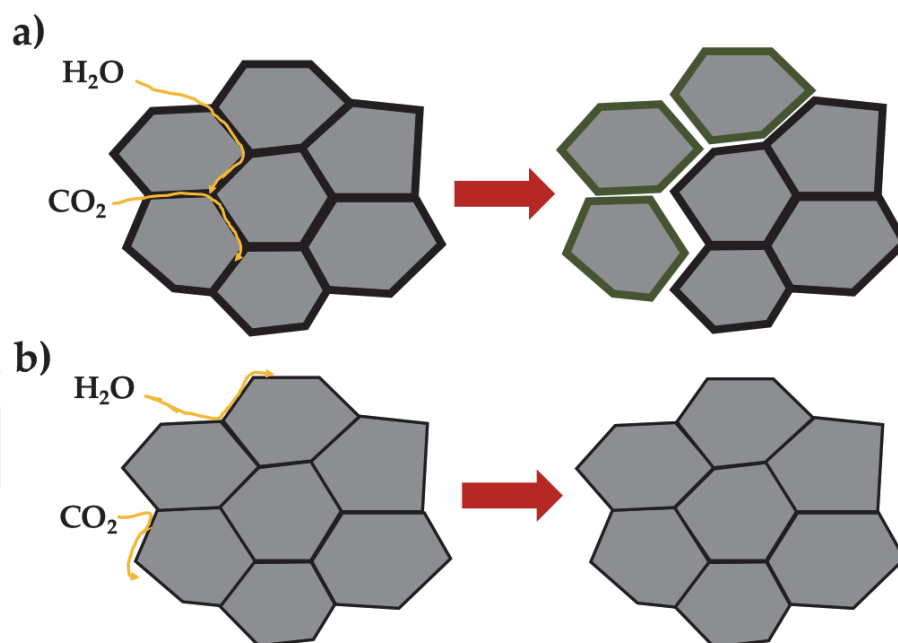
Figure 1.
Carbonate formation temperature (blue) and the conductivity isotherm at 400°C of BaCe$_{0.9}$M$_{0.1}$O$_{3-\delta}$ (M = Y, Tm, Yb, Lu, In or Sc) in moist H$_2$ as a function of the ionic radius of the dopant. Adapted from [22].

Against this scenario, one common alternative is the use of the barium zirconates or compounds containing both Ce and Zr elements, where the introduction of Zr can significantly increase their chemical stability. Nonetheless, it has also been demonstrated that increased amounts of Zr negatively impact the total conductivity of these materials, due to an increase in their refractive nature and in their grain growth, which aggravate the problem of resistive grain boundaries. As such, much lower values of total conductivity are, typically, reported for the zirconate materials than for their cerate analogues, even though their bulk protonic conductivities are actually greater [9, 26–33].

More recently, the work of Kim *et al.* [34] reported that the chemical instability of the barium cerates is due to the presence of a nanometre-thick amorphous phase found at the grain boundaries in proton-conducting BaCeO$_3$ polycrystals, which not only leads to a reduced proton mobility, but also can act as a penetration path for H$_2$O and CO$_2$ gas molecules, facilitating chemical decomposition and collapse of the microstructure (**Figure 2a**). Furthermore, this effect could be minimised by controlling the composition to obtain Ba-deficient samples in which the intergranular amorphous layer could be minimised, leading to a mitigation of the reactivity with such gases (**Figure 2b**). The presence of an amorphous layer on the interfaces between grains has also been documented in barium zirconate-based compositions [26, 35], where this feature can exert significant complications during fabrication of complete electrochemical cells [19, 36].

In summary, the high electrical conductivity and the facile processing of the doped barium cerates demands further investigation to succeed to overcome their limited stabilities. In fact, it is only very recently that research in these materials has moved towards a more fundamental and, yet, critical aspect, concerning a deeper understanding of the limiting atmospheric conditions that are necessary to retain their functionality. Taking this into account, Loureiro *et al.* [37] reanalysed the barium cerate stability limits by thermodynamic calculations, considering its decomposition products in the presence of water vapour and CO$_2$ (**Figure 3**). According to this theoretical study, no degradation would be expected for humidity values of $\sim 3 \times 10^{-2}$ atm and temperatures higher than $\sim 500°C$. However, when considering the formation of barium carbonate (**Figure 3**), the thermodynamics predict that much stricter conditions need to be applied, where only very low partial

Figure 2.
Schematic representation of microstructural changes upon reaction with water and carbon dioxide:
(a) Ba-stoichiometric compositions (thick amorphous intergranular phase); (b) Ba-deficient compositions
*(thin amorphous intergranular phase).*
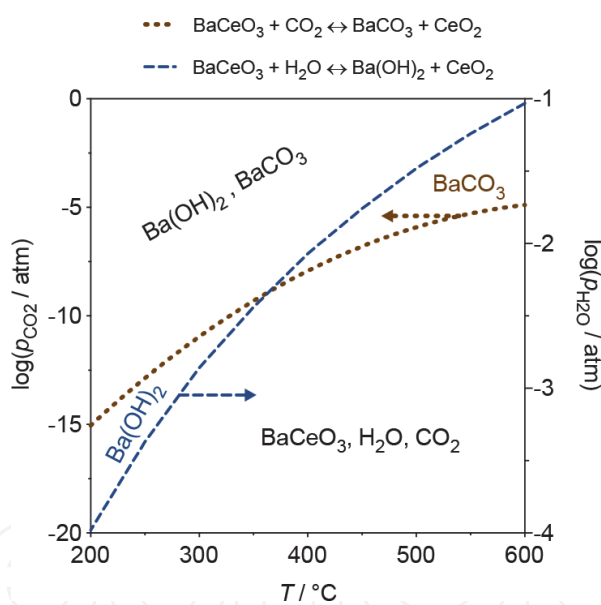
Figure 3.
Thermodynamic stability of carbon dioxide partial pressure (p_{CO_2}) and water vapour partial pressure (p_{H_2O})
as function of temperature considering the equilibrium of $BaCeO_3$ and its decomposition products (i.e. $BaCO_3$
and $Ba(OH)_2$) [38] (reproduced by permission of The Royal Society of Chemistry).

pressures of CO_2 (*e.g.* $p_{CO2} < \sim 10^{-8}$ atm at 400°C) are able to avoid barium cerate degradation.

For this reason, only very few reports can be found on successful applications of BCY membranes for chemical reactions. Most of these have concerned, ammonia synthesis [39–41], or the conversion of propane to propylene [42]. In these cases, no chemical instability has been reported and the survival of the BCY material is likely to be related to the effective absence of CO_2 or significant water vapour in these operations. To understand this further, **Figure 4** presents the maximum water vapour partial pressure (p_{H2O}) that could be tolerated in different carbonaceous atmospheres to provide an equilibrium partial pressure of CO_2 that remains below
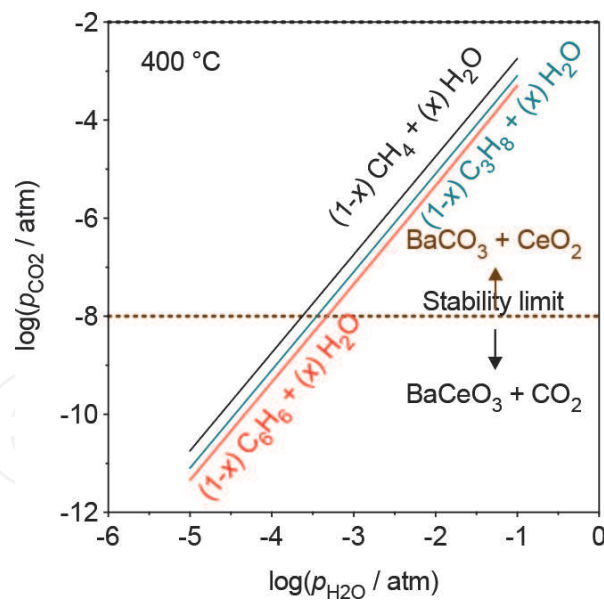
Figure 4.
Thermodynamic equilibrium for the formation of carbon dioxide from a hydrocarbon-based mixture and water at 400°C [38] (reproduced by permission of The Royal Society of Chemistry).

that of the BCY stability limit. These results demonstrate that, for example, at 400° C, these values should range between the values of $10^{-3} < p_{H2O} < \sim 10^{-4}$ atm in order to avoid decomposition of the perovskite phase, for the potential hydrocarbon atmospheres of CH_4, C_3H_8 or C_6H_6 [43].

Nonetheless, one of the requirements for operating in such low water vapour partial pressures is that the protonic conductivity must be maintained in order to ensure the functionality of the electrolyte membrane in these applications. In this respect, protonic conductors are complex materials as they are capable to offer mixed conductivity (protonic, oxide-ion and electronic), depending on the temperature and on the nature of the surrounding atmosphere [37, 38]. One of the most promising compositions for this type of application is that of the yttrium-doped barium cerate, $BaCe_{1-x}Y_xO_{3-\delta}$ (BCY), which has very high protonic conductivity at lower temperatures under humidified atmospheres (*e.g.* $\sim 10^{-3}$ S cm^{-1} at 400°C, $p_{H2O} \sim 10^{-2}$ atm) [1, 38].

Therefore, the current chapter will be focus on the electrochemical transport properties of the $BaCe_{0.9}Y_{0.1}O_{3-d}$ (BCY10) in reducing and oxidising conditions when operating in very low humidity levels. The aim of this chapter is to comprehensively explain the working limits of BCY10 and to assess its applicability as an electrolyte membrane for fuel cell, electrolysers and other electrochemical-based applications, with special focus on operation under low water vapour partial pressures.

2. Electrochemical properties of BCY10 in nominally dry reducing conditions

Figure 5 depicts the total conductivity of BCY10 analysed by impedance spectroscopy between 100 and 500°C in H_2, 10%H_2-N_2 and N_2, highlighting that no significant differences can be observed in the conductivity measured under these atmospheres. In addition, at the higher temperature range, a notable decrease of the activation energy is observed in all cases, as a result of the exsolution of protons from the structure of BCY10, and the concomitant decrease of the protonic contribution to the electrical transport [37]. Interestingly, and also surprisingly at first
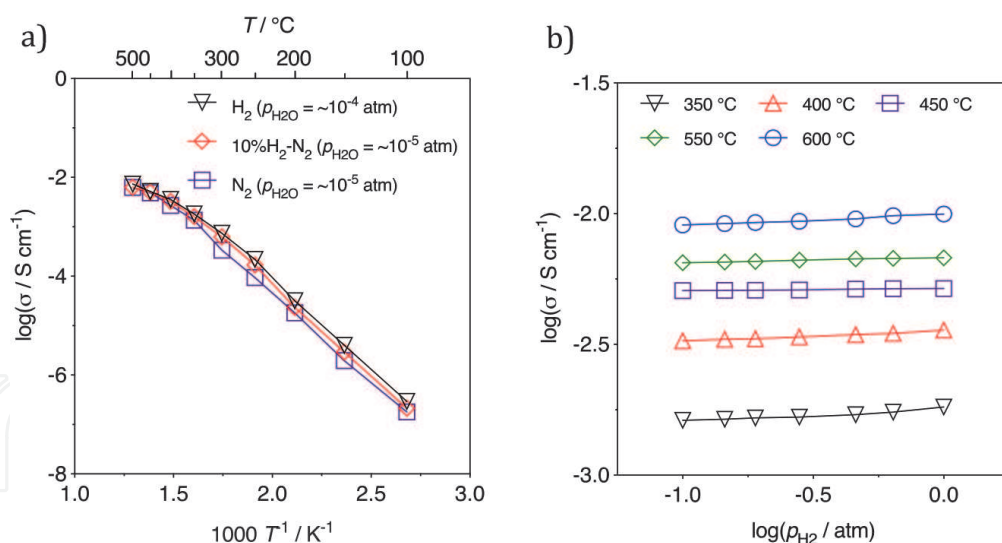
Figure 5.
(a) Temperature dependency of the total conductivity of BCY10 obtained in the temperature range 100–500°C in nominally dry conditions for H_2, 10% H_2-N_2 and N_2; (b) BCY10 total conductivity as function of hydrogen partial pressure (p_{H_2}) under nominally dry conditions in the temperature range of 350–600°C [37] (reproduced by permission of The Royal Society of Chemistry).

| Conductivity (S cm^{-1})	p_{H2O} (atm)	Reference
3.59×10^{-3}	$\sim 10^{-5}$ atm (dry H_2)	[37]
2.67×10^{-3}	$\sim 10^{-2}$ atm (wet H_2)	[14]
1.85×10^{-3}		[17]
1.96×10^{-3}		[15]
2.60×10^{-3}		[16]
8.48×10^{-4}		[18]

Table 1.
Comparison of literature studies of total conductivity of BCY10 in nominally dry and wet H_2 at 400°C [37] (reproduced by permission of The Royal Society of Chemistry).

sight, current results of total conductivity in nominally dry H_2 are close to those corresponding to the available data in literature for humidified H_2 (**Table 1**).

To analyse the contribution of electronic conductivity to this material in nominally dry conditions, the total conductivity was also analysed as a function of hydrogen partial pressure (p_{H_2}) [37], as shown in **Figure 5b**. A slight increase in total conductivity can be observed towards higher p_{H_2} values.

To be able to understand this behaviour, firstly the potential for an electronic component to conductivity must be assessed. In reducing conditions (*e.g.* H_2-containing atmospheres), the cerium cations from the B-site of the perovskite structure of BCY10 can reduce from a higher oxidation state, Ce^{4+}, to a lower one, Ce^{3+}, altering the contribution of the concentration of the electronic charge carriers. This phenomenon is well documented in the literature for various cerium-based compositions [37, 38, 44–47], being described as small-polaron electronic conductivity (*i.e.*, a localised, mobile electron, Ce'_{Ce}). Due to the high mobility of electronic conductors, such electronic contribution can exceed that of the ionic, under very reducing conditions and high temperatures [37, 45–47]. However, in the case of BCY10, the extent of cerium reduction has been assessed by Loureiro *et al.* [37], who performed coulometric titration measurements to study the potential role of electronic contribution in $BaCe_{0.9}Y_{0.1}O_{3-\delta}$ in reducing conditions as a function of temperature. This technique has been widely adopted to quantify the changes in the

oxygen non-stoichiometry ($\Delta\delta$), which can be associated with the reduction of Ce^{4+} to Ce^{3+}, following the equation:

$$2Ce_{Ce}^x + O_O^x \Leftrightarrow V_O^{\bullet\bullet} + 2Ce_{Ce}' + \frac{1}{2}O_2 \qquad (6)$$
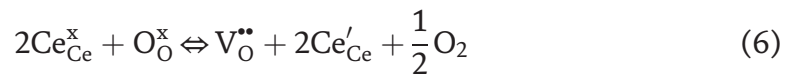
with the equilibrium constant for reduction reaction given by:

$$K_R = \frac{[V_O^{\bullet\bullet}][Ce_{Ce}']^2 p(O_2)^{\frac{1}{2}}}{[O_O^x][Ce_{Ce}^x]^2} \qquad (7)$$

The results of coulometric titration (**Figure 6**) [37] show considerable variations of $\Delta\delta$ with oxygen partial pressure only at very high temperature, with a lower impact as temperature decreases. Thus, **Figure 6** demonstrates that very extreme reducing conditions and very high temperatures are required to produce appreciable increase in the oxygen-vacancy and electronic concentrations in BCY [47, 48]. These results contrast with those of fluorite-ceria-based materials which usually show high reducibility under milder conditions [46, 49].

Thus, to take the possibility of reduction into account, the methodology applied by Loureiro *et al.* [37] for the determination of reduction equilibrium follows the method reported elsewhere [50], as described below.

The corresponding mass action constant (Eq. (7)) can be combined with the electroneutrality condition:

$$2[V_O^{\bullet\bullet}] + [OH_O^\bullet] \approx [Y_{Ce}'] + [Ce_{Ce}'] \qquad (8)$$

and other mass and lattice position restrictions, on neglecting defect interactions and assuming nearly ideal behaviour, with the following relations between the concentrations of relevant species, stoichiometric changes ($\Delta\delta$), and fraction of trivalent additive (x):

$$[Ce_{Ce}'] = \frac{Z}{v_0}(2\Delta\delta) \qquad (9)$$
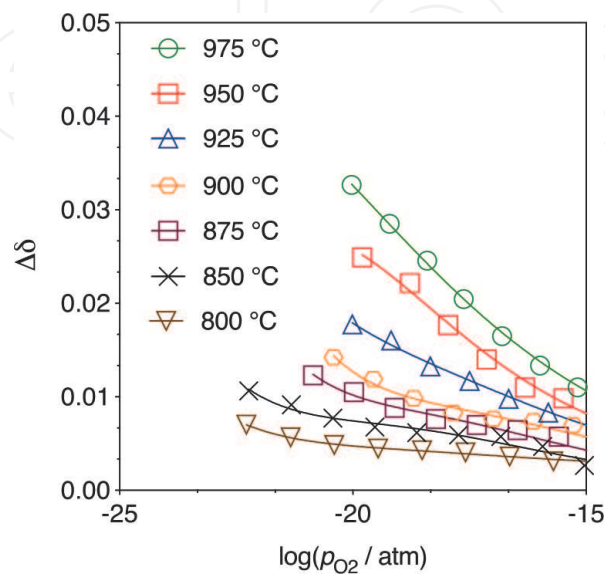
Figure 6.
Oxygen non-stoichiometry as function of oxygen partial pressure (p_{O_2}) [37] (reproduced by permission of The Royal Society of Chemistry).

$$[V_O^{\bullet\bullet}] = \frac{Z}{v_0}\left(\Delta\delta + \frac{x}{2}\right) \tag{10}$$

$$[Ce_{Ce}^x] = \frac{Z}{v_0}(1 - x - 2\Delta\delta) \tag{11}$$

$$[O_O^x] = \frac{Z}{v_0}\left(3 - \frac{x}{2} - \Delta\delta\right) \tag{12}$$

where Z is the number of atoms per unit cell and n_0, the unit cell volume. Substitution in Eq. (7) leads to the values of the equilibrium constant for reduction (K_R) from the entire range of values of $\Delta\delta$ *versus* p_{O_2} at a given temperature T:

$$K_R(T) = \frac{4\Delta\delta^2\left(\Delta\delta + \frac{x}{2}\right)p_{O_2}^{1/2}}{\left(3 - \frac{x}{2} - \Delta\delta\right)(1 - x - 2\Delta\delta)^2} \tag{13}$$

The following equation was then determined to describe the temperature dependence of K_R, from the results of oxygen-nonstoichiometry shown in **Figure 6**:

$$K_R(T) = 4.47 \cdot 10^{14} \exp\left(-7.85 \cdot 10^4/T\right) atm^{1/2} \tag{14}$$

with an enthalpy for reduction, ΔH_R = 804.99 kJ mol^{-1}. This value is significantly higher than those obtained by other authors for fluorite ceria-based materials (**Table 2**) [46, 49], underscoring the low reducibility of BCY10 in such conditions from intermediate to low temperatures.

On the basis of these results, the potential rehydration of the BCY10 material was then assessed by thermogravimetric experiments [37]. **Figure 7** depicts the concentration of protonic charge carriers as a function of temperature, calculated from the following methodology.

By expressing the equilibrium constant for water incorporation reaction (Eq. (3)) in terms of entropy, ΔS_w, and enthalpy, ΔH_w:

$$K_w = \exp\left(\frac{\Delta S_w}{R}\right) \cdot \exp\left(-\frac{\Delta H_w}{RT}\right) \tag{15}$$

where T and R have usual meanings. Given Eq. (1) and knowing that the number of oxygen sites per formula unit of barium cerate is restricted to 3, implying the site restriction relationship:

Compound	δh_r (kJ mol^{-1})	Reference
$BaCe_{0.9}Y_{0.1}O_{3-x/2-\Delta\delta}$	805	[37]
$Ce_{0.9}Gd_{0.1}O_{2-x/2-\Delta\delta}$	410–420	[46]
	438	[51]
$Ce_{0.8}Gd_{0.2}O_{2-x/2-\Delta\delta}$	430	[46]
	385	[51]
$Ce_{0.9}Sm_{0.1}O_{2-x/2-\Delta\delta}$	400	[52]
$Ce_{0.8}Sm_{0.2}O_{2-x/2-\Delta\delta}$	385	[52]
	375	[49]

Table 2.
Enthalpy (ΔH_R) for reduction of different ceria-based based solid solutions materials.
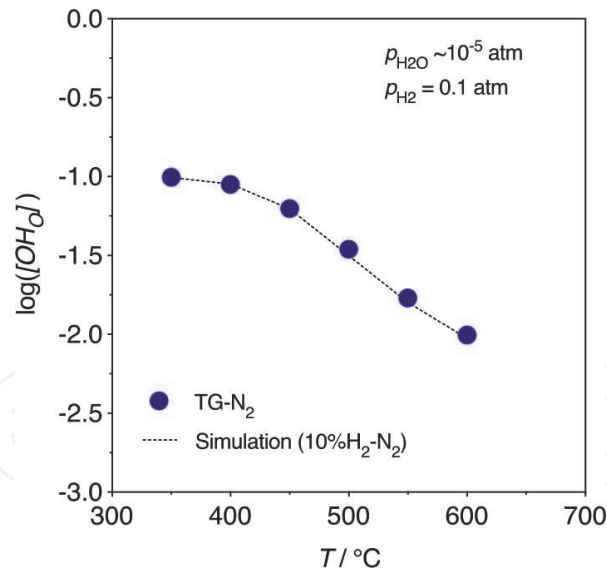
Figure 7.
Concentration protonic defects obtained from TG in N_2 and from the simulation performed in [37]
(reproduced by permission of The Royal Society of Chemistry).

$$2[V_O^{\bullet\bullet}] + [OH_O^{\bullet}] + [O_O^x] = 3 \tag{16}$$

with Eqs. (3), (15), (16), K_w can be reformulated as

$$K_w = \exp\left(\frac{4[OH_O^{\bullet}]^2}{p_{H2O}(S - [OH_O^{\bullet}])(6 - S - [OH_O^{\bullet}])}\right) \tag{17}$$

and then, the concentration of protonic defects is given by

$$[OH_O^{\bullet}] = \frac{3.K' - \sqrt{9K' - 6K'.S + K'.S^2 + 24S - 4S^2}}{K' - 4} \tag{18}$$

where $K' = K_w.p_{H2O}$ and S = [Y_{Ce}']. Because the formation of protonic defects is usually accompanied by a significant weight increase, the concentration of protonic defects as a function of temperature and water vapour partial pressure is generally measured by thermogravimetric analysis (TG). From **Figure 7**, one can observe an increase in the concentration of protonic species as a function of decreasing temperature, even in nominally dry 10%H_2/N_2. This factor is most likely related to the intrinsic formation of water vapour under the presence of hydrogen and oxygen impurities in the feed stream:

$$H_{2(g)} + \frac{1}{2}O_{2(g)} \leftrightarrow H_2O_{(g)} \tag{19}$$

This result emphasises the existence of protonic conductivity in nominally dry hydrogen-containing atmospheres, as even trace amounts of oxygen can form water vapour, potentially contributing to the hydration of the BCY10 material. Hence, the partial conductivities can be obtained by combining the results from both coulombic titration and TG experiments using a defect chemistry methodology [37].

Figure 8 shows the partial conductivities of all species (protons, oxide-ions and electrons) obtained at the temperature range (350–600°C) in nominally dry H_2 ($p_{H2O} \sim 10^{-4}$ atm). One can observe a dominance of the ionic charge carriers over the electronic carriers in the whole temperature range, corroborating the negligible reducibility of cerium cations measured by coulombic titration (**Figure 6**).
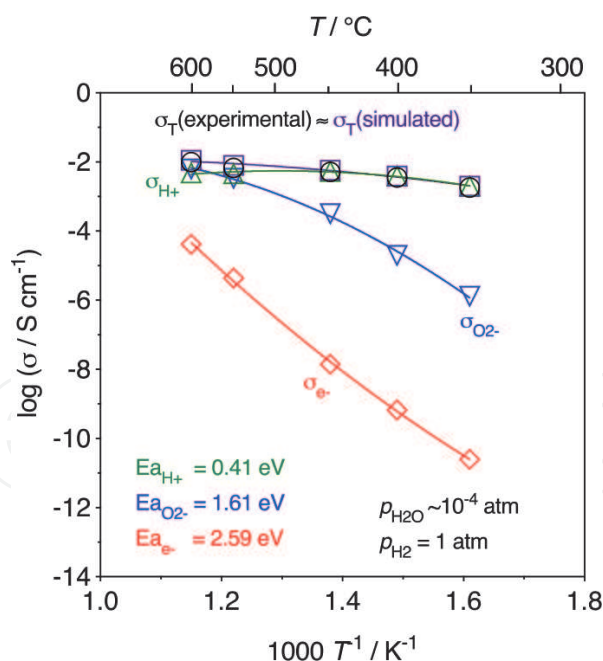
Figure 8.
Total (experimental and calculated) and partial conductivities vs. temperature. Data obtained in the temperature range 350–600°C in nominally dry conditions [37] (reproduced by permission of The Royal Society of Chemistry).

Furthermore, at the low temperature range (350–400°C), the dominance of protonic conductivity is related to the high equilibrium constant for water incorporation in BCY10, allowing a significant hydration even at p_{H2O} values as low as $\sim 10^{-4}$ atm [53], as confirmed by TG (**Figure 7**). This behaviour also explains the slight p_{H2} dependence of conductivity shown in **Figure 5b** that is due, not to electronic behaviour, but to changes in the effective water vapour partial pressure arising from Eq. (19) and subsequent slight increase in ionic conductivity due to a higher level of hydration Eq. (18). In contrast at higher temperatures in the (550–600°C) range, oxide-ion conductivity starts to become dominant at due to the loss of protons from the structure (**Figure 7**).

3. Electrochemical properties of BCY10 in low humidity oxidising conditions

The transport numbers of BCY10 in oxidising atmospheres were firstly studied by Oishi *et al.* [54] and by Grimaud *et al.* [55]. Later, Lim *et al.* [56] determined the concentration of charge carriers in BCY10 by thermogravimetric analysis (TGA) under two different humidity conditions (dry and wet, $p_{H2O} \sim 10^{-5}$ and 10^{-3} atm, respectively). More recently, Loureiro *et al.* [38] focused on the determination of the transport properties of this composition at temperatures below 600°C and under very low humidity levels ($p_{H2O} \leq 10^{-4}$ atm).

In oxidising conditions, the absence of hydrogen species, shifts the water formation reaction, Eq. (19), away from the water product, leading to a lower intrinsic water vapour partial pressure that can, in turn, decrease the protonic transport number [38]. Therefore, at the intermediate temperature range, 350–600°C, it is necessary to externally add humidity to guarantee a sufficient level of protonic conductivity. Moreover, BCY10 is known to possess p-type electronic conductivity in oxidising atmospheres, which can importantly impact the total conductivity in these conditions [38], as expressed by

$$\frac{1}{2}O_{2(g)} + V_O^{\bullet\bullet} \longleftrightarrow O_O^x + 2h^\bullet \tag{20}$$

with the following mass action constant

$$K_O \approx \frac{[h^\bullet]^2}{[V_O^{\bullet\bullet}] \cdot p_{O2}^{1/2}} \tag{21}$$

Figure 9 shows the total conductivity of BCY10 measured in the temperature range 350–600°C in wet and low humidity O_2 and N_2. From **Figure 9**, this expected decrease in the concentration of protonic species is corroborated, as in both, N_2 and O_2, total conductivity is shown to be higher in wet conditions ($p_{H2O} \sim 10^{-3}$ atm) than in low humidity conditions ($p_{H2O} \sim 10^{-7}$ atm). It is also possible to observe that low humidity N_2 ($p_{H2O} \sim 10^{-7}$ atm) the total conductivity is lower in the whole measured temperature range in comparison to wet N_2 ($p_{H2O} \sim 10^{-3}$ atm), as a result of dehydration of the sample according to Eq. (22). In contrast, in O_2, the total conductivity in low humidity and wet conditions are similar, particularly at higher temperatures, a factor that can be explained due to the presence and dominance of p-type electronic conductivity [57, 58] (see Eq. (20)):

$$2OH_O^\bullet \Leftrightarrow H_2O + V_O^{\bullet\bullet} + O_O^x \tag{22}$$

In agreement, the presence of p-type electronic conductivity can explain the slightly higher activation energy registered in low humidity O_2, 0.49 eV, in comparison to the other studied atmospheres.

Figure 10 illustrates the partial conductivities obtained in wet ($p_{H2O} \sim 10^{-3}$ atm) and low humidity ($p_{H2O} \sim 10^{-7}$ atm) conditions in N_2 and O_2. **Figure 10a** and **b** show that in moderate wet conditions ($p_{H2O} \sim 10^{-3}$ atm) the protonic conductivity is dominating in both atmospheres with activation energies similar to that obtained for the protonic conduction ($\sim$0.4–0.5 eV) [16, 17]. In contrast, in low humidity conditions (**Figure 10c** and **d**) a drop on protonic conductivity with increasing temperature is observed, due to predominant oxide-ion conductivity in both
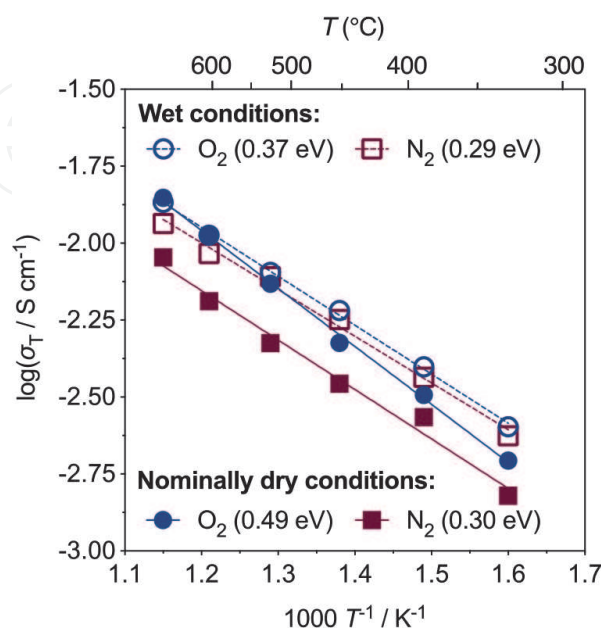
Figure 9.
Total conductivity of BCY10 in wet ($p_{H2O} \sim 10^{-3}$ atm) and low humidity ($p_{H2O} \sim 10^{-7}$ atm) N_2 and O_2. Reproduced from [38] with permission from Elsevier.
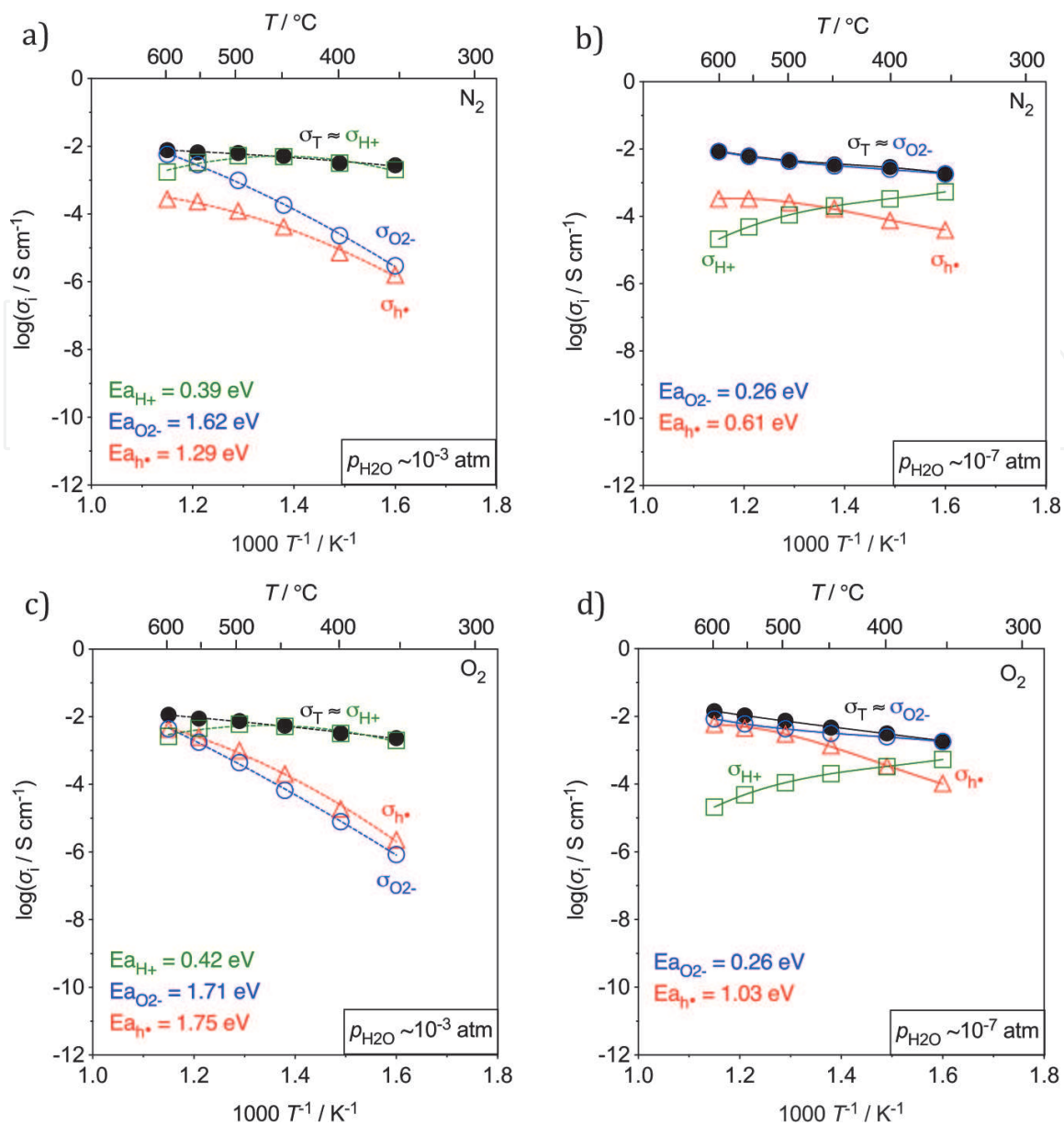
Figure 10.
*Partial conductivities obtained in wet and low humidity conditions in (a) and (b) N_2, and (c) and (d) O_2. The activation energy values, E_a, were calculated in the temperature range 350–500°C. Reproduced from [38] with permission from Elsevier.*

atmospheres. In the case of hole conductivity, the activation energies obtained were found to be lower at low humidity conditions (0.61–1.03 eV, T = 350–500°C) in comparison with those obtained in wet conditions (1.29–1.75 eV, T = 350–500°C). This can be explained by the creation of electronic defects (Eq. (20)), upon filling the oxygen vacancies.

4. Comparison between reducing and oxidising conditions under low humidity

As discussed previously, to maximise the protonic conductivity is necessary to maintain a minimum level of humidity in the order of 10^{-4}–10^{-5} atm. It is also important to emphasise that, while this level of humidity is intrinsically formed in nominally dry hydrogen-containing atmospheres, in the case of oxidising atmospheres this level must be externally supplied. A comparison of the partial conductivities in all cases is shown in **Figure 11**, for $p_{H2O} \sim 10^{-4}$ atm. At temperatures
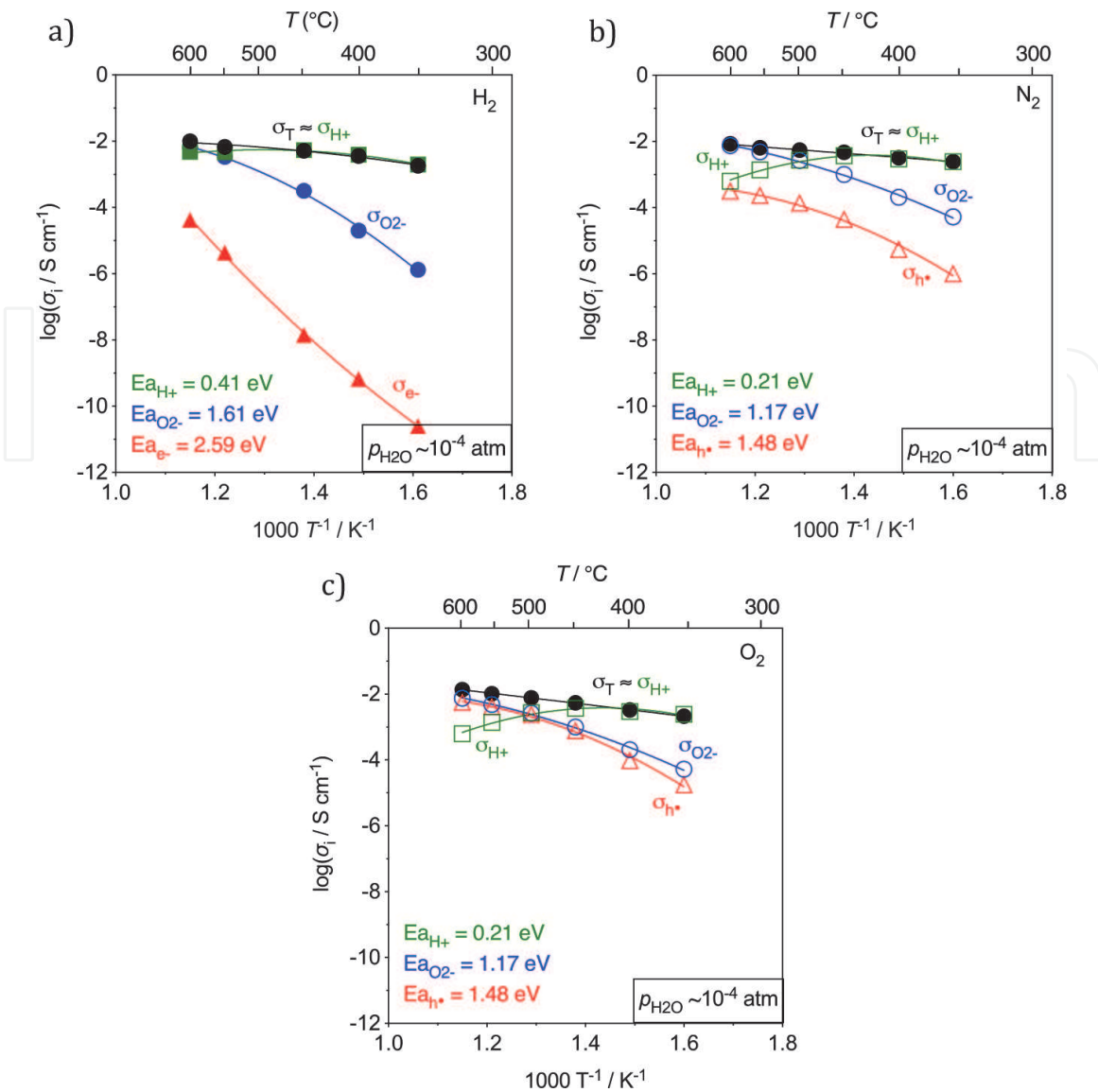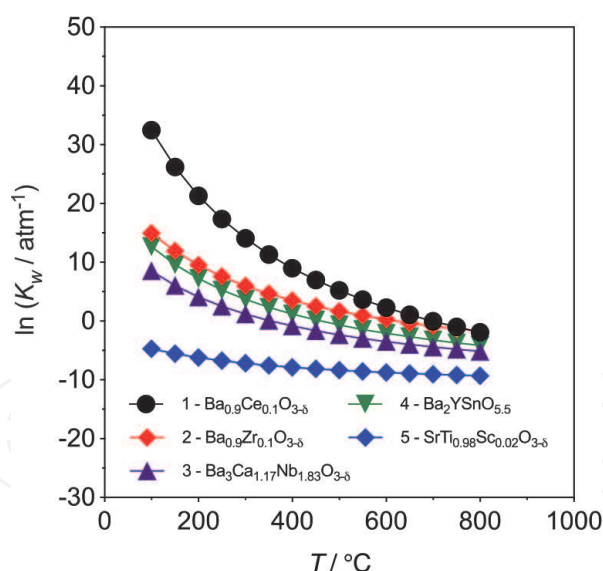
Figure 11.
Temperature dependence of partial conductivities in at $p_{H2O} \sim 10^{-4}$ *atm: (a) H_2, (b) N_2 and (c) O_2. Activation energy values, E_a, calculated in the temperature range 350-500°C. Reproduced from [38] with permission from Elsevier.*

below 450°C, the total conductivity is dominated by protonic conductivity, with the oxide-ion conductivity taking a negligible role. In contrast, at higher temperatures ($T > 450$°C), the oxide- ion conductivity dominates the total conductivity with a simultaneous decrease of protonic conductivity. With respect to the electronic conductivity, this term increases as p_{O2} increases, being only relevant in oxidising conditions and/or high temperatures. This can be explained due to the creation of electronic holes, which become more relevant with increasing p_{O2} and temperature (Eq. (20)).

Overall, BCY10 is shown to be a predominant protonic conductor in both reducing and oxidising atmospheres at sufficiently low temperatures ≤500°C, even under relatively low water vapour partial pressures ($p_{H2O} \sim 10^{-4}$–10^{-5} atm). Moreover, the level of conductivity measured at 400°C in these conditions is high, *e.g.* $\sim 10^{-3}$ S cm^{-1}. The origin of protonic conductivity is due to a high equilibrium constant for water absorption that allows this material to offer high bulk protonic conductivity at intermediate temperatures in these very low humidity conditions. From **Figure 12**, one can immediately envisage that this is a particular behaviour of BCY10 that cannot be obtained in other competing proton-conducting perovskites, due to their much lower values of K_w.

Figure 12.
Equilibrium constant for hydration of several perovskite proton conductors. Adapted from [9].

Type	Reaction	$\Delta H^0_{298}/\text{kJ mol}^{-1}$
Dehydrogenations	$2CH_{4(g)} \rightleftharpoons C_2H_{4(g)} + 2H_{2(g)}$	202
	$6CH_{4(g)} \rightleftharpoons C_6H_{6(g)} + 9H_{2(g)}$	89
	$C_3H_{8(g)} \rightleftharpoons C_3H_{6(g)} + H_{2(g)}$	124.3
	$iC_4H_{10(g)} \rightleftharpoons iC_4H_{8(g)} + H_{2(g)}$	122
	$C_8H_{10(g)} \rightleftharpoons C_8H_{8(g)} + H_{2(g)}$	117.6
Hydrogenations	$C_{10}H_{8(g)} + 2H_{2(g)} \rightleftharpoons C_{10}H_{12(g)}$	−134
	$C_6H_{10(g)} + H_{2(g)} \rightleftharpoons C_6H_{12(g)}$	−120
	$C_6H_{6(g)} + 3H_{2(g)} \rightleftharpoons C_6H_{12(g)}$	−207
	$N_{2(g)} + 3H_{2(g)} \rightleftharpoons 2NH_{3(g)}$	−109

Reproduced from [38] with permission from Elsevier.

Table 3.
Examples of dehydrogenation/hydrogenation reactions that can occur at very low humidity conditions.

This is a very exciting result since it opens a wide range of possibilities for using the BCY material, in particular, in different applications that involve very low humidity levels and low temperatures of operation. The most well-known is that of ammonia electrochemical synthesis [39–41], although many other processes concerning hydrogenation and de-hydrogenation reactions can also be considered that agree with these operating conditions (**Table 3**).

5. Conclusions

The current chapter highlights that the transport properties of $BaCe_{0.9}Y_{0.1}O_{3-\delta}$ (BCY10) in very low humidity conditions are dependent on the nature of the surrounding atmosphere and on the temperature, being significantly different in reducing and oxidising conditions and at high and low temperatures. In reducing conditions, BCY10 shows a very high protonic conductivity (*e.g.* $\sim 10^{-3}$ S cm^{-1}) at

low temperatures *i.e.* $< 400°C$, even in nominally dry atmospheres with negligible oxide-ion/electronic influence.

In the other hand, in oxidising conditions, the same behaviour can only be obtained by externally supplying humidity in the range ($p_{\text{H2O}} \sim 10^{-4}\text{–}10^{-5}$ atm) at low temperatures $\leq 500°C$. At higher temperatures, at this low humidity, the onset of hole conductivity can be noted at higher oxygen partial pressures due partial material dehydration.

The present discussion shows the importance of controlling the humidity levels in order to maximise the protonic conductivity of BCY under operation. The very low levels of humidity required ($p_{\text{H2O}} \sim 10^{-4}\text{–}10^{-5}$ atm), to ensure predominant proton conductivity in both reducing and oxidising atmospheres at low temperatures $\leq 500°C$, are highly interesting as they highlight the possibility of using this composition in applications where low humidity levels and temperatures are required, such as the suggested de-hydrogenation/hydrogenation chemical reactions, while maintaining its stability against decomposition.

Acknowledgements

Author details

Laura I.V. Holz, Vanessa C.D. Graça, Francisco J.A. Loureiro* and Duncan P. Fagg
Mechanical Engineering Department, Centre for Mechanical Technology and Automation, University of Aveiro, Aveiro, Portugal

*Address all correspondence to: francisco.loureiro@ua.pt

IntechOpen

References

[1] Morejudo SH, Zanón R, Escolástico S, Yuste-Tirados I, Malerød-Fjeld H, Vestre PK, et al. Direct conversion of methane to aromatics in a catalytic co-ionic membrane reactor. Science (80-) [Internet]. 2016 Aug 5;353(6299):563 LP – 566. Available from: http://science.sciencemag.org/content/353/6299/563.abstract

[2] Bi L, Boulfrad S, Traversa E. Steam electrolysis by solid oxide electrolysis cells (SOECs) with proton-conducting oxides. Chem Soc Rev [Internet]. 2014; 43(24):8255–70. Available from: http://dx.doi.org/10.1039/C4CS00194J

[3] Fabbri E, Bi L, Pergolesi D, Traversa E. Towards the Next Generation of Solid Oxide Fuel Cells Operating Below 600 °C with Chemically Stable Proton-Conducting Electrolytes. Adv Mater [Internet]. 2012;24(2):195–208. Available from: http://dx.doi.org/10.1002/adma.201103102

[4] Bannykh A V, Kuzin BL. Electrical conductivity of BaCe0.9Nd0.1O3−α in H2+H2O+Ar gas mixture. Ionics (Kiel) [Internet]. 2003;9(1):134–9. Available from: https://doi.org/10.1007/BF02376550

[5] Kuzin BL, Beresnev SM, Bannykh A V, Perfil'yev M V. Transport numbers of H+ and O2- in the electrochemical system (H2 + H2O),Me/BaCe0.9Nd0.1O3-α/Me,(H2 + H2O). Russ J Electrochem [Internet]. 2000;36(4):424–30. Available from: https://doi.org/10.1007/BF02756951

[6] Qiu L-G, Ma G-L, Wen D-J. Properties and Application of Ceramic BaCe0.8Ho0.2O3−α. Chinese J Chem [Internet]. 2005 Dec 22;23(12):1641–5. Available from: https://doi.org/10.1002/cjoc.200591641

[7] Virkar AN, Maiti HS. Oxygen ion conduction in pure and yttria-doped barium cerate. J Power Sources [Internet]. 1985;14(4):295–303. Available from: http://www.sciencedirect.com/science/article/pii/0378775385800458

[8] Suksamai W, Metcalfe IS. Measurement of proton and oxide ion fluxes in a working Y-doped BaCeO3 SOFC. Solid State Ionics [Internet]. 2007;178(7):627–34. Available from: http://www.sciencedirect.com/science/article/pii/S0167273807000549

[9] Kreuer KD. Proton conducting oxides. Annu Rev Mater Res. 2003 Aug; 33(1):333–59.

[10] Malavasi L, Fisher CAJ, Islam MS. Oxide-ion and proton conducting electrolyte materials for clean energy applications: structural and mechanistic features. Chem Soc Rev [Internet]. 2010;39(11):4370–87. Available from: http://dx.doi.org/10.1039/B915141A

[11] Fabbri E, D'Epifanio A, Di Bartolomeo E, Licoccia S, Traversa E. Tailoring the chemical stability of Ba (Ce0.8-xZrx)Y0.2O3-d protonic conductors for Intermediate Temperature Solid Oxide Fuel Cells (IT-SOFCs). Solid State Ionics. 2008;179 (15–16):558–64.

[12] Brett DJL, Atkinson A, Brandon NP, Skinner SJ. Intermediate temperature solid oxide fuel cells. Chem Soc Rev [Internet]. 2008;37(8):1568–78. Available from: http://dx.doi.org/10.1039/B612060C

[13] Liu M, Lynch ME, Blinn K, Alamgir FM, Choi Y. Rational SOFC material design: new advances and tools. Mater Today [Internet]. 2011;14(11):534–46. Available from: http://www.sciencedirect.com/science/article/pii/S1369702111702796

[14] Coors WG, Readey DW. Proton Conductivity Measurements in Yttrium Barium Cerate by Impedance Spectroscopy. J Am Ceram Soc [Internet]. 2004 Dec 20;85(11):2637–40. Available from: http://www3.interscience.wiley.com/journal/118935979/abstract

[15] Ma G, Shimura T, Iwahara H. Simultaneous doping with La3+ and Y3+ for Ba2+ − and Ce4+ −sites in BaCeO3 and the ionic conduction. Solid State Ionics. 1999;120(1):51–60.

[16] Kreuer KD, Dippel T, Baikov YM, Maier J. Water solubility, proton and oxygen diffusion in acceptor doped BaCeO3: A single crystal analysis. Solid State Ionics [Internet]. 1996;86–88, Par: 613–20. Available from: http://www.sciencedirect.com/science/article/pii/0167273896002214

[17] Bonanos N, Ellis B, Knight KS, Mahmood MN. Ionic conductivity of gadolinium-doped barium cerate perovskites. Solid State Ionics [Internet]. 1989;35(1–2):179–88. Available from: http://www.sciencedirect.com/science/article/pii/0167273889900283

[18] Slade RCT, Singh N. The perovskite-type proton-conducting solid electrolyte BaCe0.90Y0.10O3−α in high temperature electrochemical cells. Solid State Ionics [Internet]. 1993;61(1–3): 111–4. Available from: http://www.sciencedirect.com/science/article/pii/016727389390342Z

[19] Fabbri E, Pergolesi D, Traversa E. Materials challenges toward proton-conducting oxide fuel cells: a critical review. Chem Soc Rev [Internet]. 2010; 39(11):4355–69. Available from: http://dx.doi.org/10.1039/B902343G

[20] Fabbri E, Pergolesi D, Traversa E. Electrode materials: a challenge for the exploitation of protonic solid oxide fuel cells. Sci Technol Adv Mater [Internet].

2010 Aug 10;11(4):44301. Available from: http://www.ncbi.nlm.nih.gov/pmc/articles/PMC5090333/

[21] Kruth A, Irvine JTS. Water incorporation studies on doped barium cerate perovskites. Solid State Ionics. 2003;162–163:83–91.

[22] Matsumoto H, Kawasaki Y, Ito N, Enoki M, Ishihara T. Relation Between Electrical Conductivity and Chemical Stability of BaCeO3-Based Proton Conductors with Different Trivalent Dopants. Electrochem Solid-State Lett [Internet]. 2007 Apr 1;10(4):B77–80. Available from: http://esl.ecsdl.org/content/10/4/B77.abstract

[23] Eriksson Andersson AK, Selbach SM, Grande T, Knee CS. Thermal evolution of the crystal structure of proton conducting BaCe0.8Y0.2O3-[small delta] from high-resolution neutron diffraction in dry and humid atmosphere. Dalt Trans [Internet]. 2015;44(23):10834–46. Available from: http://dx.doi.org/10.1039/C4DT03948C

[24] Lacz A. Effect of microstructure on chemical stability and electrical properties of BaCe0.9Y0.1O3 {\thinspace}−{\thinspace}$δ$. Ionics (Kiel) [Internet]. 2016;22(8):1405–14. Available from: http://dx.doi.org/10.1007/s11581-016-1665-6

[25] Li Y, Su P-C, Wong LM, Wang S. Chemical stability study of nanoscale thin film yttria-doped barium cerate electrolyte for micro solid oxide fuel cells. J Power Sources [Internet]. 2014; 268:804–9. Available from: http://www.sciencedirect.com/science/article/pii/S0378775314009926

[26] Sun Z, Fabbri E, Bi L, Traversa E. Lowering grain boundary resistance of BaZr0.8Y0.2O3-[small delta] with LiNO3 sintering-aid improves proton conductivity for fuel cell operation. Phys Chem Chem Phys [Internet]. 2011;

13(17):7692–700. Available from: http://dx.doi.org/10.1039/C0CP01470B

[27] Donglin H, Naoyuki H, Tetsuya U. Chemical Expansion of Yttrium-Doped Barium Zirconate and Correlation with Proton Concentration and Conductivity. J Am Ceram Soc [Internet]. 2016 Jun 30; 99(11):3745–53. Available from: https://doi.org/10.1111/jace.14377

[28] Muccillo R, Muccillo ENS, Andrade TF, Oliveira OR. Thermal analyses of yttrium-doped barium zirconate with phosphor pentoxide, boron oxide and zinc oxide addition. J Therm Anal Calorim [Internet]. 2017; 130(3):1791–9. Available from: https://doi.org/10.1007/s10973-017-6523-x

[29] Narendar N, Mather GC, Dias PAN, Fagg DP. The importance of phase purity in Ni–BaZr0.85Y0.15O3−δ cermet anodes – novel nitrate-free combustion route and electrochemical study. RSC Adv [Internet]. 2013;3(3): 859–69. Available from: http://dx.doi.org/10.1039/C2RA22301E

[30] Soares HS, Zhang X, Antunes I, Frade JR, Mather GC, Fagg DP. Effect of phosphorus additions on the sintering and transport properties of proton conducting BaZr0.85Y0.15O3−δ. J Solid State Chem [Internet]. 2012;191:27–32. Available from: http://www.sciencedirect.com/science/article/pii/S0022459612001557

[31] Yang T, Loureiro FJAFJA, Queirós RP, Pukazhselvan D, Antunes I, Saraiva JAJA, et al. A detailed study of hydrostatic press, sintering aids and temperature on the densification behavior of Ba(Zr,Y)O₃₋ₐelectrolyte. Int J Hydrogen Energy. 2016;41(27): 1–10.

[32] Bozza F, Bator K, Kubiak WW, Graule T. Effects of Ni doping on the sintering and electrical properties of BaZr0.8Y0.2O3−δ proton conducting electrolyte prepared by Flame Spray

Synthesis. J Eur Ceram Soc [Internet]. 2016;36(1):101–7. Available from: http://www.sciencedirect.com/science/article/pii/S0955221915301291

[33] Grant H, Anthony M, G. CW, Sandrine R. Chemical expansion in BaZr0.9−xCexY0.1O3−δ (x = 0 and 0.2) upon hydration determined by high-temperature X-ray diffraction. J Am Ceram Soc [Internet]. 2017 Oct 7; 101(3):1298–309. Available from: https://doi.org/10.1111/jace.15275

[34] Kim H-S, Bae H Bin, Jung W, Chung S-Y. Manipulation of Nanoscale Intergranular Phases for High Proton Conduction and Decomposition Tolerance in BaCeO3 Polycrystals. Nano Lett [Internet]. 2018 Feb 14;18(2):1110–7. Available from: https://doi.org/10.1021/acs.nanolett.7b04655

[35] Park J-S, Lee J-H, Lee H-W, Kim B-K. Low temperature sintering of BaZrO3-based proton conductors for intermediate temperature solid oxide fuel cells. Solid State Ionics [Internet]. 2010;181(3):163–7. Available from: http://www.sciencedirect.com/science/article/pii/S0167273809002549

[36] Loureiro FJA, Nasani N, Reddy GS, Munirathnam NR, Fagg DP. A review on sintering technology of proton conducting BaCeO3-BaZrO3 perovskite oxide materials for Protonic Ceramic Fuel Cells. J Power Sources [Internet]. 2019;438:226991. Available from: http://www.sciencedirect.com/science/article/pii/S037877531930984X

[37] Loureiro FJA, Pérez-Coll D, Graça VCD, Mikhalev SM, Ribeiro AFG, Mendes A, et al. Proton conductivity in yttrium-doped barium cerate in nominally dry reducing conditions for application in chemical synthesis. J Mater Chem A [Internet]. 2019;7: 18135–42. Available from: submitted

[38] Loureiro FJA, Ramasamy D, Ribeiro AFG, Mendes A, Fagg DP.

Underscoring the transport properties of yttrium-doped barium cerate in nominally dry oxidising conditions. Electrochim Acta [Internet]. 2019;334: 135625. Available from: https://doi.org/10.1016/j.electacta.2020.135625

[39] Otomo J, Noda N, Kosaka F. Electrochemical Synthesis of Ammonia with Proton Conducting Solid Electrolyte Fuel Cells at Intermediate Temperatures. ECS Trans [Internet]. 2015 Jun 2;68(1): 2663–70. Available from: http://ecst.ecsdl.org/content/68/1/2663.abstract

[40] Li Z, Liu R, Wang J, Xu Z, Xie Y, Wang B. Preparation of double-doped BaCeO3 and its application in the synthesis of ammonia at atmospheric pressure. Sci Technol Adv Mater [Internet]. 2007;8(7–8):566–70. Available from: http://www.sciencedirect.com/science/article/pii/S1468699607001404

[41] Marnellos G, Stoukides M. Ammonia Synthesis at Atmospheric Pressure. Science (80-) [Internet]. 1998 Oct 2;282(5386):98 LP – 100. Available from: http://science.sciencemag.org/content/282/5386/98.abstract

[42] Feng Y, Luo J, Chuang KT. Propane Dehydrogenation in a Proton-conducting Fuel Cell. J Phys Chem C [Internet]. 2008 Jul 1;112(26):9943–9. Available from: http://dx.doi.org/10.1021/jp710141c

[43] Bale CW, Bélisle E, Chartrand P, Decterov SA, Eriksson G, Gheribi AE, et al. FactSage thermochemical software and databases, 2010–2016. Calphad [Internet]. 2016;54:35–53. Available from: http://www.sciencedirect.com/science/article/pii/S0364591616300694

[44] Bonanos N, Willy Poulsen F. Considerations of defect equilibria in high temperature proton-conducting cerates. J Mater Chem [Internet]. 1999;9 (2):431–4. Available from: http://dx.doi.org/10.1039/A805150J

[45] Pérez-Coll D, Aguadero A, Núñez P, Frade JR. Mixed transport properties of Ce1−xSmxO2−x/2 system under fuel cell operating conditions. Int J Hydrogen Energy [Internet]. 2010;35(20):11448–55. Available from: http://www.sciencedirect.com/science/article/pii/S0360319910009900

[46] Pérez-Coll D, Marrero-López D, Ruiz-Morales JC, Núñez P, Abrantes JCC, Frade JR. Reducibility of Ce1−xGdxO2−δ in prospective working conditions. J Power Sources [Internet]. 2007;173(1):291–7. Available from: http://www.sciencedirect.com/science/article/pii/S0378775307009044

[47] Bonanos N. Transport study of the solid electrolyte BaCe0.9Gd0.1O2.95 at high temperatures. J Phys Chem Solids [Internet]. 1993;54(7):867–70. Available from: http://www.sciencedirect.com/science/article/pii/002236979390258S

[48] Chen W, Nijmeijer A, Winnubst L. Oxygen non-stoichiometry determination of perovskite materials by a carbonation process. Solid State Ionics [Internet]. 2012 Dec 14;229:54–8. Available from: http://www.sciencedirect.com/science/article/pii/S0167273812005723

[49] Abrantes JCC, Pérez-Coll D, Núñez P, Frade JR. Electronic transport in Ce0.8Sm0.2O1.9−δ ceramics under reducing conditions. Electrochim Acta [Internet]. 2003 Aug 15;48(19):2761–6. Available from: http://www.sciencedirect.com/science/article/pii/S0013468603003955

[50] Pérez-Coll D, Marrero-López D, Ruiz-Morales JC, Núñez P, Abrantes JCC, Frade JR. Reducibility of Ce1-xGdxO2-δ in prospective working conditions. J Power Sources. 2007;173 (1):291–7.

[51] Wang S, Inaba H, Tagawa H, Hashimoto T. Nonstoichiometry of Ce0.8Gd0.2O1.9−x . J Electrochem Soc

[Internet]. 1997 Nov 1;144(11):4076–80. Available from: http://jes.ecsdl.org/content/144/11/4076.abstract

[52] Kobayashi T, Wang S, Dokiya M, Tagawa H, Hashimoto T. Oxygen nonstoichiometry of Ce1−ySmyO2−0.5y−x (y=0.1, 0.2). Solid State Ionics [Internet]. 1999;126(3):349–57. Available from: http://www.sciencedirect.com/science/article/pii/S0167273899002593

[53] Kreuer KD. Aspects of the formation and mobility of protonic charge carriers and the stability of perovskite-type oxides. Solid State Ionics [Internet]. 1999 Oct;125(1–4):285–302. Available from: http://www.sciencedirect.com/science/article/pii/S0167273899001885

[54] Oishi M, Akoshima S, Yashiro K, Sato K, Mizusaki J, Kawada T. Defect structure analysis of B-site doped perovskite-type proton conducting oxide BaCeO3: Part 2: The electrical conductivity and diffusion coefficient of BaCe0.9Y0.1O3−δ. Solid State Ionics [Internet]. 2008;179(39):2240–7. Available from: http://www.sciencedirect.com/science/article/pii/S016727380800564X

[55] Grimaud A, Bassat JM, Mauvy F, Simon P, Canizares A, Rousseau B, et al. Transport properties and in-situ Raman spectroscopy study of BaCe0.9Y0.1O3−δ as a function of water partial pressures. Solid State Ionics [Internet]. 2011;191(1):24–31. Available from: http://www.sciencedirect.com/science/article/pii/S0167273811001767

[56] Lim D-K, Im H-N, Song S-J, Yoo H-I. Hydration of Proton-conducting BaCe0.9Y0.1O3−δ by Decoupled Mass Transport. Sci Rep [Internet]. 2017;7(1):486. Available from: http:https://dx.doi.org/10.1038/s41598-017-00595-w

[57] Heras-Juaristi G, Pérez-Coll D, Mather GC. Temperature dependence of partial conductivities of the BaZr0.7Ce0.2Y0.1O3-δ proton conductor. J Power Sources [Internet]. 2017;364:52–60. Available from: http://www.sciencedirect.com/science/article/pii/S0378775317310352

[58] Triviño-Peláez Á, Pérez-Coll D, Mather GC. Electrical properties of proton-conducting BaCe0.8Y0.2O3-δ and the effects of bromine addition. Acta Mater [Internet]. 2019;167:12–22. Available from: http://www.sciencedirect.com/science/article/pii/S1359645419300436